Quantum Physics, Data Science, Tensor Linear Modeling, and Spacekime Analytics

Ivo D. Dinov

Statistics Online Computational Resource
Health Behavior & Biological Sciences
Computational Medicine & Bioinformatics
Michigan Institute for Data Science
University of Michigan

https://SOCR.umich.edu

Joint work with Milen V. Velev (BTU) & Yueyang Shen (UM)

Based on the book *"Data Science: Time Complexity, Inferential Uncertainty & Spacekime Analytics"*

STATISTICS ONLINE COMPUTATIONAL RESOURCE (SOCR)
UNIVERSITY OF MICHIGAN

Slides Online: "SOCR News"

1

Outline

- ❑ Complex-Time (*kime*) & Rationale
- ❑ Solutions of untrahyperbolic wave equations
- ❑ Open Spacekime Problems

- ❑ Data/Neuro Science Applications
  - ❑ Random Sampling vs. Hidden Variables Paradigm
  - ❑ Neuroimaging (fMRI): time-series ➔ kime-surfaces
- ❑ Bayesian Formulation of Spacekime Inference
- ❑ Live Demo Links

2

Complex-Time (*Kime*)

- ❑ At a given spatial location, $\boldsymbol{x}$, complex time (*kime*) is defined by $\kappa = re^{i\varphi} \in \mathbb{C}$, where:
  - ❑ the <u>magnitude</u> represents the longitudinal events order ($r > 0$) and characterizes the longitudinal displacement in time, and
  - ❑ event <u>phase</u> ($-\pi \le \varphi < \pi$) is an angular displacement, event direction, or random sampling index
- ❑ There are multiple alternative parametrizations of kime in the complex plane
- ❑ Space-kime manifold is $\mathbb{R}^3 \times \mathbb{C}$:
  - ❑ $(\boldsymbol{x}, k_1)$ and $(\boldsymbol{x}, k_4)$ have the same spacetime representation, but different spacekime coordinates,
  - ❑ $(\boldsymbol{x}, k_1)$ and $(\boldsymbol{y}, k_1)$ share the same kime, but represent different spatial locations,
  - ❑ $(\boldsymbol{x}, k_2)$ and $(\boldsymbol{x}, k_3)$ have the same spatial-locations and kime-directions, but appear sequentially in order, $r_2 < r_1$.

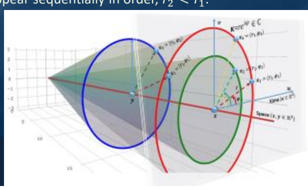

3

Rationale for *Time* → *Kime* Extension

- ❑ <u>**Math**</u> – $Time$ is a special case of *kime*, $\kappa = |\kappa|e^{i\varphi}$ where $\varphi = 0$ (nil-phase)
  - $\mathbb{R}^+$ is algebraically a *multiplicative* (algebraic) group, with multiplicative unity (identity) $= 1$, multiplicative inverses $t^{-1} = \frac{1}{t}$, and associativity law $t_1 \times (t_2 \times t_3) = (t_1 \times t_2) \times t_3$
  - The *time* domain ($\mathbb{R}^+$) is **not** a complete *algebraic field* w.r.t. $(+,\ \times)$:
    - Additive unity (0), element additive inverse $(-t)$: $t + (-t) = 0$; is outside $\mathbb{R}^+$ (time-domain)
    - $x^2 + 1 = 0$ has no solutions in time (or in $\mathbb{R}$) ….

$$\text{Group}(\times) \subseteq Ring\left(\underbrace{\overbrace{(+,*)}^{\text{Compatible operations}}}_{\text{associative \& distributive}}\right) \subseteq Field\ \overbrace{(+,*)}^{\text{Group}(+)}$$

  - Classical time ($\mathbb{R}^+$) is a *positive cone* over the field of the real numbers ($\mathbb{R}$)
  - Time forms a subgroup of the multiplicative group of the reals
  - Whereas <u>kime</u> ($\mathbb{C}$) is an algebraically *closed prime field* that naturally extends time
  - *Time* is ordered but *kime* is not! Yet, the kime magnitude preserves the intrinsic time order
  - Kime ($\mathbb{C}$) represents the smallest natural extension of time, as a complete filed that agrees with time
  - The *time* group is closed under addition, multiplication, and division (but not subtraction). It has the topology of $\mathbb{R}$ and the structure of a multiplicative topological group $\equiv$ additive topological semigroup
- ❑ <u>**Physics**</u> –
  - ❑ Problem of time … (DOI 10.1007/978-3-319-58848-3)
  - ❑ $\mathbb{R}$ and $\mathbb{C}$ Hilbert-space quantum theories make different predictions (DOI: 10.1038/s41586-021-04160-4)
- ❑ <u>**AI/Data Science**</u> – Random IID sampling, Bayesian reps, tensor modeling of $\mathbb{C}$ kimesurfaces, novel analytics

Dinov & Velev (2021)

4

Ultrahyperbolic Wave Equation – Cauchy Initial Data

- ❑ <u>**Nonlocal constraints**</u> yield the existence, uniqueness & stability of local and global solutions to the ultrahyperbolic wave equation under Cauchy initial data …

$$\underbrace{\sum_{i=1}^{d_s} \partial_{x_i}^2 u \equiv \Delta_{\boldsymbol{x}} u(\boldsymbol{x}, \boldsymbol{\kappa})}_{\text{spatial Laplacian}} = \underbrace{\Delta_{\boldsymbol{\kappa}} u(\boldsymbol{x}, \boldsymbol{\kappa}) \equiv \sum_{i=1}^{d_t} \partial_{\kappa_i}^2 u}_{\text{temporal Laplacian}}, \quad \underbrace{\left| \begin{array}{l} u_o = u\left(\underbrace{\boldsymbol{x}}_{x \in D_s}, \underbrace{0, \boldsymbol{\kappa}_{-1}}_{\kappa \in D_t}\right) = f(\boldsymbol{x}, \boldsymbol{\kappa}_{-1}) \\ u_1 = \partial_{\kappa_1} u(\boldsymbol{x}, 0, \boldsymbol{\kappa}_{-1}) = g(\boldsymbol{x}, \boldsymbol{\kappa}_{-1}) \end{array} \right.}_{\text{initial conditions (Cauchy Data)}}$$

where $\boldsymbol{x} = (x_1, x_2, \dots, x_{d_s}) \in \mathbb{R}^{d_s}$ and $\boldsymbol{\kappa} = (\kappa_1, \kappa_2, \dots, \kappa_{d_t}) \in \mathbb{R}^{d_t}$ are the Cartesian coordinates in the d_s space and d_t time dims.

Stable local solution over a Fourier frequency region defined by <u>nonlocal constraints</u> $|\boldsymbol{\xi}| \ge |\boldsymbol{\eta}_{-1}|$:

$$\hat{u}\left(\boldsymbol{\xi}, \underbrace{\kappa_1, \boldsymbol{\eta}_{-1}}_{\boldsymbol{\eta}}\right) = \cos\left(2\pi\,\kappa_1 \sqrt{|\boldsymbol{\xi}|^2 - |\boldsymbol{\eta}_{-1}|^2}\right) \underbrace{\hat{u}_o(\boldsymbol{\xi}, \boldsymbol{\eta}_{-1})}_{c_1} + \sin\left(2\pi\,\kappa_1 \sqrt{|\boldsymbol{\xi}|^2 - |\boldsymbol{\eta}_{-1}|^2}\right) \underbrace{\frac{\hat{u}_1(\boldsymbol{\xi}, \boldsymbol{\eta}_{-1})}{2\pi\sqrt{|\boldsymbol{\xi}|^2 - |\boldsymbol{\eta}_{-1}|^2}}}_{c_2},$$

where $\mathcal{F}\begin{pmatrix} u_o \\ u_1 \end{pmatrix} = \begin{pmatrix} \hat{u}_o \\ \hat{u}_1 \end{pmatrix} = \begin{pmatrix} \hat{u}_o(\boldsymbol{\xi}, \boldsymbol{\eta}_{-1}) \\ \hat{u}_1(\boldsymbol{\xi}, \boldsymbol{\eta}_{-1}) \end{pmatrix} = \begin{pmatrix} \hat{u}(\boldsymbol{\xi}, \boldsymbol{\eta}_{-1}) \\ \partial_{\kappa_1} \hat{u}(\boldsymbol{\xi}, \boldsymbol{\eta}_{-1}) \end{pmatrix}$.

$$u\left(\boldsymbol{x}, \underbrace{\kappa_1, \boldsymbol{\kappa}_{-1}}_{\boldsymbol{\kappa}}\right) = \mathcal{F}^{-1}(\hat{u})(\boldsymbol{x}, \boldsymbol{\kappa}) = \int_{\hat{D}_s \times \hat{D}_{t_{-1}}} \hat{u}(\boldsymbol{\xi}, \kappa_1, \boldsymbol{\eta}_{-1}) \times e^{2\pi i \langle x, \xi \rangle} \times e^{2\pi i \langle \kappa_{-1}, \eta_{-1} \rangle} d\boldsymbol{\xi}\, d\boldsymbol{\eta}_{-1}.$$

Craig & Weinstein (2008) | Wang et al. (2022) | Dinov & Velev (2021)

5

A *Spacekime* Solution to Wave Equation

- ❑ Math Generalizations: Derived <u>other spacekime concepts</u>: law of addition of velocities, energy-momentum conservation law, stability conditions for particles moving in spacekime, conditions for nonzero rest particle mass, causal structure of spacekime, and solutions of the ultrahyperbolic wave equation under Cauchy initial data …

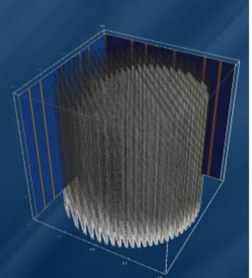

Wang et al., 2022 | Dinov & Velev (2021)

6

Math Foundations of Spacekime

- **Spacekime:** $(\boldsymbol{x},\boldsymbol{k}) = \big(\underbrace{x^1,x^2,x^3}_{\text{space}},\underbrace{c\kappa_1 = x^4, c\kappa_2 = x^5}_{\text{kime}}\big) \in X$
- **Kevents** (*complex events*): points (or states) in the spacekime manifold X. Each kevent is defined by where ($\boldsymbol{x} = (x,y,z)$) it occurs in space, what is its *causal longitudinal order* $\left(r = \sqrt{(x^4)^2+(x^5)^2}\right)$, and in what *kime-direction* ($\varphi = \text{atan2}(x^5,x^4)$) it takes place
- **Spacekime interval** (ds) is defined using the general Minkowski 5×5 metric tensor
- **Spacekime Calculus of differentiation and integration** (defined using Wirtinger derivatives and path integration
- Generalization of the **equations of motion in spacekime**
- **Lorentz transformation** (between 2 spacekime inertial frames)
- Solutions to ultrahyperbolic PDEs

Dinov & Velev (2021)

7

Spacekime Calculus

- Kime **Wirtinger derivative**, 1st order kime-derivative at $\boldsymbol{k} = (r,\varphi)$, $z = (x+iy)$:

$$f'(z) = \frac{\partial f(z)}{\partial z} = \frac{1}{2}\left(\frac{\partial f}{\partial x} - i\frac{\partial f}{\partial y}\right) \text{ and } f'(\bar{z}) = \frac{\partial f(\bar{z})}{\partial \bar{z}} = \frac{1}{2}\left(\frac{\partial f}{\partial x} + i\frac{\partial f}{\partial y}\right).$$

In Conjugate-pair basis: $df = \partial f + \bar{\partial} f = \frac{\partial f}{\partial z}dz + \frac{\partial}{\partial \bar{z}}d\bar{z}$

In Polar kime coordinates:

$$f'(k) = \frac{\partial f(k)}{\partial k} = \frac{1}{2}\left(\cos\varphi\frac{\partial f}{\partial r} - \frac{1}{r}\sin\varphi\frac{\partial f}{\partial \varphi} - i\left(\sin\varphi\frac{\partial f}{\partial r} + \frac{1}{r}\cos\varphi\frac{\partial f}{\partial \varphi}\right)\right) = \frac{e^{-i\varphi}}{2}\left(\frac{\partial f}{\partial r} - \frac{i}{r}\frac{\partial f}{\partial \varphi}\right)$$

$$f'(\bar{k}) = \frac{\partial f(\bar{k})}{\partial \bar{k}} = \frac{1}{2}\left(\cos\varphi\frac{\partial f}{\partial r} - \frac{1}{r}\sin\varphi\frac{\partial f}{\partial \varphi} + i\left(\sin\varphi\frac{\partial f}{\partial r} + \frac{1}{r}\cos\varphi\frac{\partial f}{\partial \varphi}\right)\right) = \frac{e^{i\varphi}}{2}\left(\frac{\partial f}{\partial r} + \frac{i}{r}\frac{\partial f}{\partial \varphi}\right).$$

- Kime **Wirtinger integration**:

Path-integral $\lim_{|z_{m+1}-z_m|\to 0} \sum_{m=1}^{n-1}(f(z_m)(z_{m+1}-z_m)) \cong \oint_{z_a}^{z_b} f(z)dz$.

Definite area integral: for $\Omega \subseteq \mathbb{C}$, $\int_\Omega f(z)dzd\bar{z}$.

Indefinite integral: $\int f(z)dzd\bar{z}$, $df = \frac{\partial f}{\partial z}dz + \frac{\partial f}{\partial \bar{z}}d\bar{z}$.

The *Laplacian* in terms of conjugate pair coordinates is $\Delta f = d^2 f = 4\frac{\partial f}{dz}\frac{\partial f}{d\bar{z}} = 4\frac{\partial f}{d\bar{z}}\frac{\partial f}{dz}$.

Dinov & Velev (2021)

8

Newton's equations of motion in kime

$$\left|\begin{aligned} v &= at + v_o \\ x &= x_o + v_o t + \frac{1}{2}at^2 \\ v^2 &= 2a(x-x_o) + v_o^2 \end{aligned}\right. \Rightarrow \left|\begin{aligned} v &= a_1k_1 + v_{o1} = a_2k_2 + v_{o2}, \\ x &= x_{o1} + v_{o1}k_1 + \frac{1}{2}a_1k_1^2 = x_{o2} + v_{o2}k_2 + \frac{1}{2}a_2k_2^2, \\ \sqrt{v_2^4 - v^2v_2^2} &= -a_1(x - x_{o1}) + \sqrt{v_{o2}^4 - v_o^2v_{o2}^2}, \\ \sqrt{v_1^4 - v^2v_1^2} &= -a_2(x - x_{o2}) + \sqrt{v_{o1}^4 - v_o^2v_{o1}^2} \end{aligned}\right.$$

- Derived from the Kime Wirtinger velocity and acceleration
  - Kime-velocity ($\boldsymbol{k} = (t,\varphi)$) is defined by the Wirtinger derivative of the position with respect to kime:

$$v(\boldsymbol{k}) = \frac{\partial x}{\partial \boldsymbol{k}} = \frac{1}{2}\left(\cos\varphi\frac{\partial x}{\partial t} - \frac{1}{t}\sin\varphi\frac{\partial x}{\partial \varphi} - i\left(\sin\varphi\frac{\partial x}{\partial t} + \frac{1}{t}\cos\varphi\frac{\partial x}{\partial \varphi}\right)\right)$$

  - The directional kime derivatives v_1 and v_2, (**e** = unit vector of spatial directional change):

$$\boldsymbol{v}_1 = \frac{\sqrt{dx^2+dy^2+dz^2}}{dk_1}\boldsymbol{e} = \frac{\sqrt{dx^2+dy^2+dz^2}}{\cos\varphi dt - t\sin\varphi d\varphi}\boldsymbol{e}, \quad \boldsymbol{v}_2 = \frac{\sqrt{dx^2+dy^2+dz^2}}{dk_2}\boldsymbol{e} = \frac{\sqrt{dx^2+dy^2+dz^2}}{\sin\varphi dt + t\cos\varphi d\varphi}\boldsymbol{e}$$

Dinov & Velev (2021)

9

Spacekime Generalizations

- Spacekime generalization of **Lorentz transform** between two reference frames, K & K':

(the interval ds is Lorentz transform invariant)

$$\underbrace{\begin{pmatrix} x' \\ y' \\ z' \\ k_1' \\ k_2' \end{pmatrix}}_{\in K'} = \begin{pmatrix} \zeta & 0 & 0 & -\frac{c^2}{v_1}\beta^2\zeta & -\frac{c^2}{v_2}\beta^2\zeta \\ 0 & 1 & 0 & 0 & 0 \\ 0 & 0 & 1 & 0 & 0 \\ -\frac{1}{v_1}\beta^2\zeta & 0 & 0 & 1+(\zeta-1)\frac{c^2}{(v_1)^2}\beta^2 & (\zeta-1)\frac{c^2}{v_1v_2}\beta^2 \\ -\frac{1}{v_2}\beta^2\zeta & 0 & 0 & (\zeta-1)\frac{c^2}{v_1v_2}\beta^2 & 1+(\zeta-1)\frac{c^2}{(v_2)^2}\beta^2 \end{pmatrix} \underbrace{\begin{pmatrix} x \\ y \\ z \\ k_1 \\ k_2 \end{pmatrix}}_{\in K}$$

where $0 \le \beta = \frac{1}{\sqrt{\left(\frac{c}{v_1}\right)^2 + \left(\frac{c}{v_2}\right)^2}} \le 1$ & $\zeta = \frac{1}{\sqrt{1-\beta^2}} \ge 1$.

Dinov & Velev (2021)

10

Data→Kime-Transforms→PDEs→AI

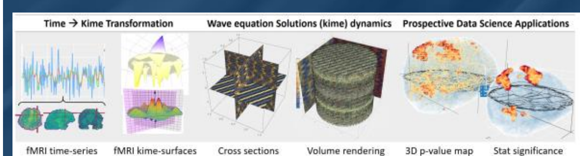

Wang et al., 2022 | Dinov & Velev (2021)

11

Hidden Variable Theory & Random Sampling

- Kime phase distributions are mostly symmetric, random observations ≡ phase sampling

https://wiki.socr.umich.edu/index.php/SOCR_EduMaterials_Activities_GeneralCentralLimitTheorem

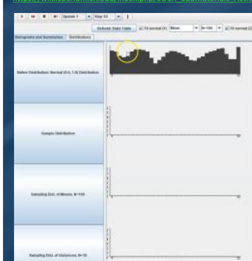

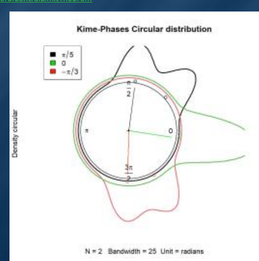

https://www.socr.umich.edu/TCIU/HTMLs/Chapter6_Kime_Phases_Circular.html

Dinov, Christou & Sanchez (2008) Dinov & Velev (2021)

12

(Many) Spacekime Open Math Problems

❑ **Ergodicity**

Let's look at particle velocities in the 4D Minkowski spacetime (X), a measure space where gas particles move spatially and evolve longitudinally in time. Let $\mu = \mu_{\boldsymbol{x}}$ be a measure on X, $f(\boldsymbol{x},t) \in L^1(X,\mu)$ be an integrable function (e.g., velocity of a particle), and $T: X \to X$ be a measure-preserving transformation at position $\boldsymbol{x} \in \mathbb{R}^3$ and time $t \in \mathbb{R}^+$.

A pointwise ergodic theorem argues that in a measure theoretic sense, the average of f (e.g., velocity) over all particles in the gas system at a fixed time, $\bar{f} = E_t(f) = \int_{\mathbb{R}^3} f(\boldsymbol{x},t)\,d\mu_{\boldsymbol{x}}$, will be equal to the average f of just one particle ($\boldsymbol{x}$) over the entire time span,

$$\tilde{f} = \lim_{n\to\infty}\left(\frac{1}{n}\sum_{m=0}^{n} f(T^m\boldsymbol{x})\right), \text{ i.e., (show) } \bar{f} \equiv \tilde{f}.$$

The spatial probability measure is denoted by $\mu_{\boldsymbol{x}}$ and the transformation $T^m\boldsymbol{x}$ represents the dynamics (time evolution) of the particle starting with an initial spatial location $T^o\boldsymbol{x} = \boldsymbol{x}$.

Investigate the ergodic properties of various transformations in the 5D **spacekime**:

$$\underbrace{\bar{f} \equiv E_\kappa(f) = \frac{1}{\mu_{\boldsymbol{x}}(X)}\int f\left(\boldsymbol{x},\underbrace{t,\phi}_{\kappa}\right)d\mu_{\boldsymbol{x}}}_{\text{space averaging}} \stackrel{?}{=} \underbrace{\lim_{t\to\infty}\left(\frac{1}{t}\sum_{m=0}^{t}\left(\int_{-\pi}^{+\pi} f(T^m\boldsymbol{x},t,\phi)\,d\Phi\right)\right) \equiv \tilde{f}}_{\text{kime averaging}}$$

Dinov & Velev (2021)

13

Mathematical-Physics ⟹ Data Science & AI

Physics	Data/Neuro Sciences
A **particle** is a small localized object that permits observations and characterization of its physical or chemical properties	An **object** is something that exists by itself, actually or potentially, concretely or abstractly, physically or incorporeal (e.g., person, subject, etc.)
An **observable** a dynamic variable about particles that can be measured	A **feature** is a dynamic variable or an attribute about an object that can be measured
Particle **state** is an observable particle characteristic (e.g., position, momentum)	**Datum** is an observed quantitative or qualitative value, an instantiation, of a feature
Particle **system** is a collection of independent particles and observable characteristics, in a closed system	**Problem**, aka Data System, is a collection of independent objects and features, without necessarily being associated with a priori hypotheses
Wave-function	**Inference-function**
Reference-Frame **transforms** (e.g., Lorentz)	Data **transformations** (e.g., wrangling, log-transform)
State of a system is an observed measurement of all particles ~ wavefunction	**Dataset (data)** is an observed instance of a set of datum elements about the problem system, $\boldsymbol{O} = \{X, Y\}$
A **particle system is computable** if (1) the entire system is logical, consistent, complete and (2) the unknown internal states of the system don't influence the computation (wavefunction, intervals, probabilities, etc.)	**Computable data object** is a very special representation of a dataset which allows direct application of computational processing, modeling, analytics, or inference based on the observed dataset
…	…

14

Mathematical-Physics ⟹ Data Science & AI

Physics	Data Science
Wavefunction Wave equ problem: $\left(\frac{\partial^2}{\partial x^2} - \frac{1}{v^2}\frac{\partial^2}{\partial t}\right)\psi(x,t) = 0$ Complex Solution: $\psi(x,t) = Ae^{i(kx-wt)}$ where $\left\|\frac{w}{k}\right\| = v$, represents a traveling wave	*Inference function* - describing a solution to a specific data analytic system (a problem). For example, • A linear (GLM) model represents a solution of a prediction inference problem, $\boldsymbol{Y} = \boldsymbol{X}\beta$, where the inference function quantifies the effects of all independent features ($\boldsymbol{X}$) on the dependent outcome ($\boldsymbol{Y}$), data: $\boldsymbol{O} = \{\boldsymbol{X},\boldsymbol{Y}\}$: $\psi(\boldsymbol{O}) = \psi(\boldsymbol{X},\boldsymbol{Y}) \Rightarrow \hat{\beta} = \hat{\beta}^{OLS} = \langle X\|X\rangle^{-1}\langle X\|Y\rangle = \left(X^TX\right)^{-1}X^TY.$ • A non-parametric, non-linear, alternative inference is SVM classification. If $\psi_x \in \boldsymbol{H}$, is the lifting function $\psi: R^\eta \to R^d$ ($\psi: x \in R^\eta \to \tilde{x} = \psi_x \in \boldsymbol{H}$), where $\eta \ll d$, the kernel $\psi_x(y) = \langle x\|y\rangle: \boldsymbol{O} \times \boldsymbol{O} \to \boldsymbol{R}$ transformes non-linear to linear separation, the observed data $\boldsymbol{O}_i = \{x_i, y_i\} \in R^\eta$ are lifted to $\psi_{\boldsymbol{O}_i} \in \boldsymbol{H}$. Then, the SVM prediction operator is the weighted sum of the kernel functions at $\psi_{\boldsymbol{O}_i}$, where $\boldsymbol{\beta}^*$ is a solution to the SVM regularized optimization: $\langle\psi_O \| \beta^*\rangle_H = \sum_{i=1}^{n} p_i^*\langle\psi_O\|\psi_{O_i}\rangle_H$ The linear coefficients, p_i^*, are the dual weights that are multiplied by the label corresponding to each training instance, $\{y_i\}$. Inference always depends on the (input) data; however, it does not have 1-1 and onto bijective correspondence with the data, since the inference function quantifies predictions in a probabilistic sense.

GLM/SVM: https://DSPA.predictive.space | Dinov, Springer (2018)

15

Spacekime Analytics: fMRI Example

❑ 3D Isosurface Reconstruction of (2D *space* × 1D *time*) fMRI signal

Spacetime Reconstruction using trivial phase-angle; kime=time=(magnitude, 0) | Spacekime Reconstruction using correct kime=(magnitude, phase)

3D pseudo-spacetime reconstruction:

$$f = \hat{h}\,(\underbrace{x_1, x_2}_{space},\ \underbrace{t}_{time})$$

16

Spacekime Analytics: Kime-series = Surfaces (not curves)

In the 5D spacekime manifold, time-series curves extend to kime-series, i.e., surfaces parameterized by kime-magnitude (t) and the kime-phase (φ)

Kime-phase aggregating operators that can be used to transform standard time-series curves to spacekime kime-surfaces, which can be modeled, interpreted, and predicted using advanced spacekime analytics

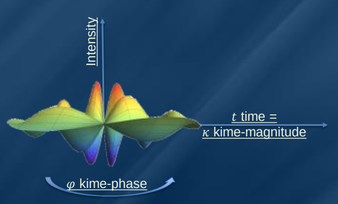

17

Spacetime Time-series ⟹ *Spacekime Kimesurfaces* ⟹ *TLM*

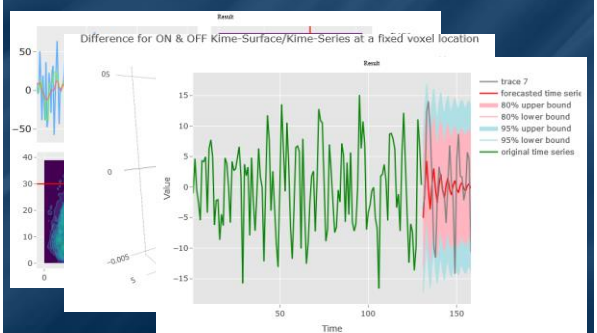

Zhang et al., 2022 | Dinov & Velev (2021)

18

Mapping Longitudinal Data (Time-series) to Kime-Surfaces

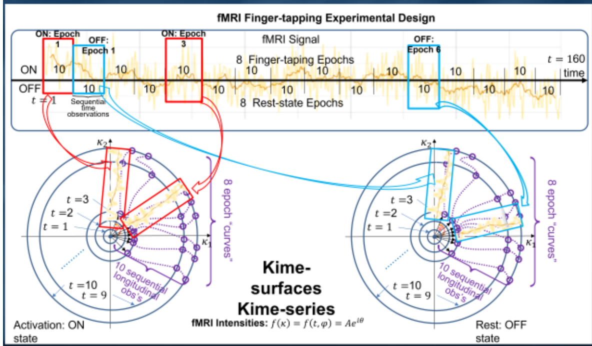

Zhang et al., 2022 | Dinov & Velev (2021)

20

Mapping Longitudinal Data (Time-series) to Kime-Surfaces

The *forward* and *inverse* (continuous) Laplace transforms are defined below.

- For a given function (of time) $f(t): \mathbb{R}^+ \to \mathbb{C}$, the **Laplace transform** is the function of a complex frequency argument, $F(z) = \mathcal{L}(f)(z): \mathbb{C} \to \mathbb{C}$:
$$\mathcal{L}(f)(z) = F(z) = \int_0^{\infty} f(t)e^{-zt}dt\,.$$
- For a given function of a complex frequency argument, $F(z)$, the **Inverse Laplace transform** (ILT) is the function of a positive real (time-like) argument $f(t) = \mathcal{L}^{-1}(F)(t): \mathbb{R}^+ \to \mathbb{C}$, which is defined in terms of a complex path integral (a.k.a. Bromwich integral or Fourier–Mellin integral):
$$f(t) = \mathcal{L}^{-1}(F)(t) = \frac{1}{2\pi i}\lim_{T\to\infty}\int_{\gamma-iT}^{\gamma+iT} e^{zt}F(z)dz\,,$$

where the parameter $\gamma \in \mathbb{R}$ is chosen so that the entire complex contour path of the integral is inside of the region of convergence of $F(z)$.

In probability and statistics, the Laplace transform plays the role of expected value. If X is a random variable, then its Laplace transform, i.e., the LT of its probability density function f_X, is given by the expectation of an exponential: $\mathcal{L}(X) = \mathcal{L}(f)(z) = \mathbb{E}(e^{-zX})$.

Zhang et al., 2022 | Dinov & Velev (2021)

21

Mapping Longitudinal Data (Time-series) to Kime-Surfaces

Apply the ILT ($\mathcal{L}^{-1}$) to reconstruct a time-series, $\hat{f}(t) = \mathcal{L}^{-1}(F)(t)$:

$$F(z) = \mathcal{L}(f) = \underbrace{\frac{1}{z+1}}_{F_1(z)=\mathcal{L}(f_1(t)=e^{-t})} + \underbrace{\frac{1}{z^2+1}}_{F_2(z)=\mathcal{L}(f_2(t)=\sin(t))} \times \underbrace{\frac{z}{z^2+1}}_{F_3(z)=\mathcal{L}(f_3(t)=\cos(t))} + \underbrace{\frac{1}{z^2}}_{F_4(z)=\mathcal{L}(f_4(t)=t)}\,,$$

$$f(t) = \mathcal{L}^{-1}(F) = \mathcal{L}^{-1}(F_1 + F_2 \times F_3 + F_4)) =$$

$$\mathcal{L}^{-1}(F_1) + \Big(\underbrace{\mathcal{L}^{-1}(F_2) * \mathcal{L}^{-1}(F_3)}_{\text{convolution}}\Big)(t) + \mathcal{L}^{-1}(F_4) =$$

$$\mathcal{L}^{-1}(\mathcal{L}(f_1))(t) + \Big(\mathcal{L}^{-1}(\mathcal{L}(f_2)) * \mathcal{L}^{-1}(\mathcal{L}(f_3))\Big)(t) + \mathcal{L}^{-1}(\mathcal{L}(f_4))(t)\,,$$

$$f(t) = \mathcal{L}^{-1}(F)(t) = f_1(t) + (f_2 * f_3)(t) + f_4(t) =$$

$$e^{-t} + \int_0^t \sin(\tau) \times \cos(t-\tau)d\tau + t = t + e^{-t} + \frac{t\sin(t)}{2}\,.$$

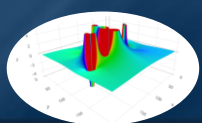

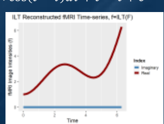

Zhang et al., 2022 | Dinov & Velev (2021)

22

2D Fourier Transform – The Importance of Magnitudes & Phases

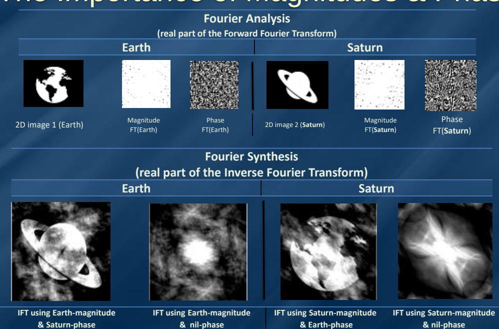

23

Tensor-based Linear Modeling of fMRI

3-Step Analysis: registering the fMRI data into a brain atlas space, 56 ROIs, tensor linear modeling, post-hoc FDR processing & selection of large clusters of significant voxels are identified within the important ROIs: $Y = \underbrace{\langle X, B\rangle}_{\text{tensor product}} + E$.

The dimensions of the time-tensor Y are $\overbrace{160}^{\text{time}} \times \overbrace{a \times b \times c}^{\text{ROI b-box}}$, where the tensor elements represent the response variable $Y[t, x, y, z]$, i.e., fMRI intensity. For fMRI magnitude (real-valued signal), the design kime-tensor X dimensions are: $\underbrace{10 * 8}_{\text{Kime}(\text{Time}*e^{i\times Repeat})} \times \underbrace{State}_{\text{Stim vs. Rest (2)}} \times \underbrace{4}_{\text{effects}} \times \underbrace{1}_{\mathbb{R}}$.

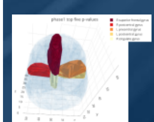

Step 1: ROI analysis

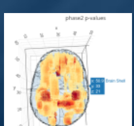

Step 2: Voxel analysis

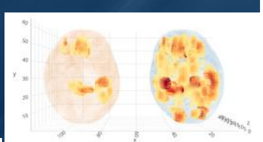

Voxel-based TLM/Analysis Corrected (step 3, left) vs. Raw (step 2, right)

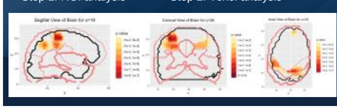

Step 3: 2D voxel analysis projections (finger-tapping task modeling)

24

Bayesian Inference Representation

- Suppose we have a single spacetime observation $X = \{x_{i_o}\} \sim p(x \mid \gamma)$ and $\gamma \sim p(\gamma \mid \varphi = \text{phase})$ is a process parameter (or vector) that we are trying to estimate.
- Spacekime analytics aims to make appropriate inference about the process X.
- The sampling distribution, $p(x \mid \gamma)$, is the distribution of the observed data X conditional on the parameter γ and the prior distribution, $p(\gamma \mid \varphi)$, of the parameter γ before the data X is observed, $\varphi = \text{phase aggregator}$.
- Assume that the hyperparameter (vector) φ, which represents the kime-phase estimates for the process, can be estimated by $\hat{\varphi} = \varphi'$.
- Such estimates may be obtained from an oracle (model distribution), approximated using similar datasets, acquired as phases from samples of analogous processes, derived via some phase-aggregation strategy, or computed via Laplace transform.
- Let the posterior distribution of the parameter γ given the observed data $X = \{x_{i_o}\}$ be $p(\gamma|X, \varphi')$ and the process parameter distribution of the kime-phase hyperparameter vector φ be $\gamma \sim p(\gamma \mid \varphi)$.

25

Bayesian Inference Simulation

- Simulation example using 2 random samples drawn from mixture distributions each of $n_A = n_B = 10K$ observations:
  - $\{X_{A,i}\}_{i=1}^{n_A}$, where $X_{A,i} = 0.3U_i + 0.7V_i$, $U_i \sim N(0,1)$ and $V_i \sim N(5,3)$, and
  - $\{X_{B,i}\}_{i=1}^{n_B}$, where $X_{B,i} = 0.4P_i + 0.6Q_i$, $P_i \sim N(20,20)$ and $Q_i \sim N(100,30)$.
- The intensities of cohorts A and B are independent and follow different mixture distributions. We'll split the first cohort (A) into training (C) and testing (D) subgroups, and then:
  - Transform all four cohorts into Fourier k-space,
  - Iteratively randomly sample single observations from the (training) cohort C,
  - Reconstruct the data into spacetime using a single kime-magnitude value and alternative kime-phase estimates derived from cohorts B, C, and D, and
  - Compute the classical spacetime-derived population characteristics of cohort A and compare them to their spacekime counterparts obtained using a single C kime-magnitude paired with B, C, or D kime-phases.

29

Bayesian Inference Simulation

Summary statistics for the original process (cohort A) and the corresponding values of their counterparts computed using the spacekime reconstructed signals based on kime-phases of cohorts B, C, and D. The estimates for the latter three cohorts correspond to reconstructions using a single spacetime observation (i.e., single kime-magnitude) and alternative kime-phase priors (in this case, kime-phases derived from cohorts B, C, and D).

	Spacetime	Spacekime Reconstructions (single kime-magnitude)		
Summaries	**(A)** **Original**	(B) Phase=Diff. Process	(C) Phase=True	(D) Phase=Independent
Min	-2.38798	-3.798440	-2.98116	-2.69808
1st Quartile	-0.89359	-0.636799	-0.76765	-0.76453
Median	0.03311	0.009279	-0.05982	-0.08329
Mean	**0.00000**	**0.000000**	**0.00000**	**0.00000**
3rd Quartile	0.75772	0.645119	0.72795	0.69889
Max	3.61346	3.986702	3.64800	3.22987
Skewness	0.348269	0.001021943	0.2372526	0.31398
Kurtosis	**-0.68176**	**0.2149918**	**-0.4452207**	**-0.3270084**

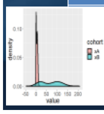

30

Bayesian Inference Simulation

The correlation between the original data (A) and its reconstruction using a single kime magnitude and the correct kime-phases (C) is $\rho(A,C) = 0.89$.

This strong correlation suggests that a substantial part of the A process energy can be recovered using only a single observation. In this case, to reconstruct the signal back into spacetime and compute the corresponding correlation, we used a single kime-magnitude (sample-size=1) and process C kime-phases.

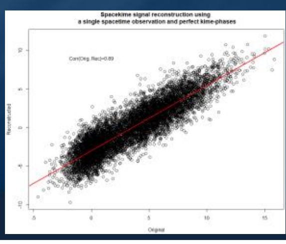

31

Bayesian Inference Simulation

Let's demonstrate the Bayesian inference corresponding to this spacekime data analytic problem using a simulated bimodal experiment:

$X_A = 0.3U + 0.7V$, where $U \sim N(0,1)$ and $V \sim N(5,3)$

Specifically, we will illustrate the Bayesian inference using repeated single spacetime observations from cohort A, $X = \{x_{i_o}\}$, and varying kime-phase priors (θ = phase aggregator) obtained from cohorts B, C, or D, using different posterior predictive distributions.

Relations between the empirical data distribution (dark blue) and samples from the posterior predictive distribution, representing Bayesian simulated spacekime reconstructions (light-blue). The derived Bayesian estimates do not perfectly match the empirical distribution of the simulated data, yet there is clearly information encoding that is captured by the spacekime data reconstructions.

This signal compression can be exploited by subsequent model-based or model-free data analytic strategies for retrospective prediction, prospective forecasting, ML classification, AI derived clustering, and other spacekime inference methods.

32

Bayesian Inference Simulation

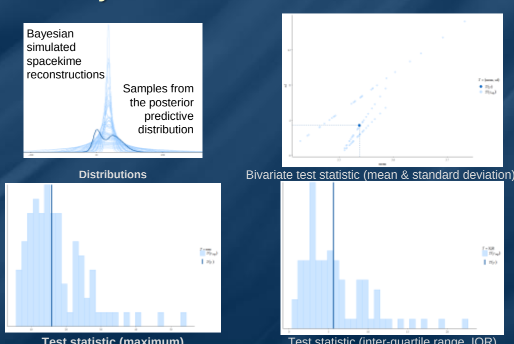

Relations between the empirical data distribution (dark blue) and samples from the posterior predictive distribution, Bayesian simulated spacekime reconstructions (light-blue).

33

Spacekime Analytics: Resources & Demos

- Tutorials
  - https://TCIU.predictive.space
  - https://SpaceKime.org
- R Package
  - https://cran.rstudio.com/web/packages/TCIU
- GitHub
  - https://github.com/SOCR/TCIU
- Pubs
  - https://socr.umich.edu/people/dinov/publications.html

34

Acknowledgments

Slides Online: "SOCR News"

Funding

NIH: UL1 TR002240, R01 CA233487, R01 MH121079, R01 MH126137, T32 GM141746
NSF: 1916425, 1734853, 1636840, 1416953, 0716055, 1023115

Collaborators

- **SOCR: Milen Velev, Yueyang Shen, Daxuan Deng, Zijing Li, Yongkai Qiu, Zhe Yin, Yufei Yang, Yuxin Wang, Rongqian Zhang, Yuyao Liu, Yupeng Zhang, Yunjie Guo, Simeone Marino**
- **UMich DCMB/MIDAS/MCAIM Centers**: Josh Welch, Maryam Bagherian, Lydia Bieri, Kayvan Najarian, Chris Monk, Issam El Naqa, Brian Athey

https://SOCR.umich.edu

35

36